Multivariate analysis of flood characteristics in a climate change context of the watershed of the Baskatong reservoir, Province of Québec, Canada

M.-A. Ben Aissia* [1]

F. Chebana [1]

T. B. M. J. Ouarda [1]

L. Roy [2]

G. Desrochers [3]

I. Chartier [3]

É. Robichaud [2]

[1] Hydro-Québec/NSERC Chair in Statistical Hydrology, Canada Research Chair on the Estimation of Hydrological Variables, INRS-ETE,
490, de la Couronne, Quebec, (Quebec)
Canada, G1K 9A9.

[2] Hydro-Québec Équipement
855, Ste-Catherine East, 19th Floor, Montreal (Quebec)
Canada, H2L 4P5.

[3] Institut de Recherche d'Hydro-Quebec
1800 Montee Ste-Julie, Varennes (Québec)
Canada, J3X 1S1

* Corresponding author: mohamed.ben.aissia@ete.inrs.ca

February 2011

Revised version submitted to Hydrological Processes

Abstract

The analysis of the impact of climate change (CC) on flood peaks has been the subject of several studies. However, a flood is characterized not only by its peak, but also by other characteristics such as its volume and duration. Little effort has been directed towards the study of the impact of CC on these characteristics. The aim of the present study is to evaluate and compare flood characteristics in a CC context, in the watershed of the Baskatong reservoir (Province of Québec, Canada). Comparisons are based on observed flow data and simulated flow series obtained from hydrological models using meteorological data from a regional climate model for a reference period (1971-2000) and a future period (2041-2070). To this end, two hydrological models HSAMI and HYDROTEL are considered. Correlations, stationarity, change-points and the multivariate behavior of flood series were studied. The results show that, at various levels, all flood characteristics could be affected by CC.

1. Introduction and literature review

Governments and populations are increasingly interested in the impacts of global warming. According to the World Meteorological Organization (WMO), the frequency of extreme events has doubled in last years (Pachauri, 2002). Among these phenomena we mention the strong growth of hurricanes in Europe (category 5) in 2005 as well as the prolonged heat waves in Europe during the summer of 2003 (see e.g. Beniston, 2004 and Wilkinson and Souter, 2008).

Climate Change (CC), caused by increased concentrations of greenhouse gases, has effects on the hydrological cycle. Impacts on the frequencies and intensities of rainfall are expected. Water quality is also supposed to be degraded as it is directly related to the available water quantity (Arnell, 1999; Warren, 2004). In the province of Québec, Canada, many environmental and industrial sectors may suffer from CC, such as: forest harvesting, hydropower generation, coastal erosion control, aquatic ecosystems protection, water management, agriculture, transportation, human health and tourism (see e.g., Bergeron et al., 1997).

In order to identify and study the effects of CC on the hydrologic regime in the province of Québec and other northern countries, a number of hydrological variables were the subject of several studies (e.g., Ouarda et al., 1999; Seidou and Ouarda, 2007; Khaliq et al., 2008 and Saint-Laurent et al., 2009). These studies showed the existence of breaking points, trends of average and/or variance and cyclical evolution in various hydrological variables.

Other studies focused on the comparison of the outputs of global climate models

coupled with hydrological models, reanalysis results or historical data (e.g., Singh, 1987; Mortsch and Quinn, 1996 and Guay et al., 2004). These studies showed an increase in annual average temperatures that promotes evaporation and increases the contribution of precipitations. On the other hand, studies of CC effects on solid precipitations showed that there could be a decrease in the fraction of solid precipitations (e.g., Bruce et al., 2000; Dibike and Coulibaly, 2005; and EEA., 2008). For the mean annual flow, various studies provided that it might be affected (increase or decrease) in the future (e.g., D'Arcy et al., 2005; Graham et al., 2007 and Mareuil et al., 2007). Studies of the effects of CC on the low water level showed that it could be reduced in the future (e.g., Guay et al., 2004; Minville et al., 2008 and Vescovi et al., 2008). Mortsch and Quinn (1996), Lorrain (2007) and Vescovi et al. (2008) studied the effects of CC on winter and spring flows. Contrary to low water level, these studies concluded that winter and spring flows would be sustained over the coming decades.

Frequencies and magnitudes of extreme events are of great importance in studies of climate change effects on hydrology in the province of Québec and other northern regions (e.g., Mareuil et al., 2007). These studies pointed out potential increases in the flow volume and flow peak. The effects of CC on the spring flood could be expressed by an advance of its starting date (e.g., Mareuil et al., 2007; Fortin et al., 2007 and Vescovi et al., 2008) and a decrease in its peak (e.g., Doré et al., 2006 and Minville et al., 2008).

The impact of CC on flood peak has been the subject of several studies. However,

floods are characterized not only by their peak (Q_p), but also by the following characteristics: starting date (*ds*), ending date (*de*), peak date (*dp*), duration (*D*), volume (*V*), climb-rate (T_m) and shape of the hydrograph (F_h). Little efforts have been directed towards the study of the impact of CC simultaneously on all these characteristics.

The aim of the present study is to assess and compare the aforementioned flood characteristics in a CC context. To this end, we considered the watershed of the Baskatong reservoir (Province of Québec, Canada). Observed and simulated flow data of this basin are employed to obtain all the above flood characteristics on reference and future periods. Furthermore, two hydrological models, HSAMI and HYDROTEL, are considered in order to evaluate sensitivity of the estimation of the flood characteristics regarding the choice of hydrological model. In addition, the followed methodology is composed by several parts including descriptive statistical analysis, correlation study, stationarity testing, detection of break-points of all series and multivariate analysis of the main characteristic.

The paper is organized as follows. The study area, the available data as well as the different employed methods are presented in section 2. Section 3 presents the study results. The conclusions are presented in Section 4.

2. Data series and methodology

In the present section, we introduce the study area and we describe the different methods to evaluate and to analyze the considered flood characteristics.

101 The study area is the watershed of the Baskatong reservoir located in the province of
102 Québec in Canada (see Figure 1). The watershed has an area of 13 040 km^2. The
103 hydrological regime is dominated by snowmelt runoff, which occurs generally from
104 April to June. The Mercier dam, at the outlet of the Baskatong reservoir, is the largest
105 structure in the watershed. The regularization of Mercier dam is controlled by
106 Hydro-Quebec, a public utility in Québec responsible for electricity generation and
107 supply.
108 The flood characteristics are evaluated and compared using three categories of
109 datasets from Baskatong watershed. The first category consists in the observed flow
110 series from January 1st 1969 to December 31st 2000. In the second category, there are
111 two simulated flow data sets obtained by the hydrological models HSAMI (Bisson
112 and Roberge, 1983) and HYDROTEL (Fortin et al., 1995). The inputs of these models
113 are meteorological data. These data are simulated by the Canadian Regional Climate
114 Model (CRCM) using the atmospheric fields from ERA-40 reanalysis as boundary
115 conditions on the period from January 1st 1969 to December 31st 2000. In the third
116 category, there are two simulated flow data sets obtained by HSAMI and
117 HYDROTEL using the direct method on the period from January 1st 1961 to
118 December 31st 2070. For these series, we used the results of the CRCM (e.g., Brochu
119 and Laprise, 2007 and Music and Caya, 2007) driven by the atmospheric fields from
120 Coupled Global Climate Model (CGCM3), run #4 on the assumption of an increase in
121 greenhouse gases for the A2 scenario.
122 For comparison of flood characteristics in CC context, we used two periods of

thirty years:

- Reference period: from January 1st 1971 to December 31st 2000;
- Future period: from January 1st 2041 to December 31st 2070.

The choice of the last thirty years is explained by the fact that, over thirty years, the extended average of long-term climatic cycles such as the El Niño-Southern Oscillation (ENSO) is taken into account in the series. It follows that for the three categories of data we have seven sets of thirty years. The description of these seven sets and the corresponding notations are summarized in Table 1.

2.1 Determination of flood characteristics

As indicated in the introduction, a flood is described by several characteristics throughout a hydrograph. Figure 2 illustrates a typical hydrograph and the different characteristics. In the present study, analyses are focused on spring flood characteristics, resulting mainly from snowmelt, whereas for fall flood only the peak flow is considered. In the following, we give the definition of each flood characteristic as well as the corresponding determination methods from flow series.

Starting and ending dates:

Starting date *« ds »* and ending date *« de »* of flood are the most important characteristics since they affect the determination of the remaining characteristics. To calculate these two characteristics, we use the method proposed by Pacher (2006). It is based on the analysis of cumulative annual hydrographs by adjusting the slopes with a linear approximation.

Flood duration:

Once the starting and ending dates are obtained, the duration « D » is defined by the number of days between the starting date and ending date, i.e., $D = de - ds$.

Flood peak:

For the determination of flood peak « Q_p », we use the idea of the Flood-Duration-Frequency (QdF) approach (Cunderlik and Ouarda, 2006) to reduce the 1-day flood peak uncertainty. The method consists in determining the flood peak of the day « i » as the maximum of the « n » flood peaks averages around « i ». From a practical point of view, it is more reasonable to take small values of «n». Indeed, with a large value of n, we will be more close to the volume concept. In the present study we considered $n = 3$. The corresponding flood peak is then:

$$Q_p = max\{q_{i3}, i = d_s, .., d_e\} \quad (1)$$

where q_{i3} is the flow of the day « d_i » associated to 3 days given by $q_{i3} = mean\{q_{i-1}, q_i, q_{i+1}\}$ with q_i is the flow of the day « d_i ».

Peak of fall flood:

For the fall flood, the flood peak « Q_{pa} » is the maximum flow between July 1st and December 31st. It is determined by:

$$Q_{pa} = max\{q_{i3}, i = d_1, .., d_n\} \quad (2)$$

where d_1 and d_n represent July 1st and December 31st respectively.

Peak date:

The peak date « d_p » is the date that corresponds to flood peak « Q_p ».

Flood volume:

168 The volume «*V*» is determined by the following equation:

169 $$V = \sum_{i=d_s}^{d_e} q_i \qquad (3)$$

170 where q_i is the flow of the day « d_i ».

171 *Hydrograph shape « F_h »:*

172 The shape of the hydrograph can be obtained on the basis of the date of flood
173 peak « d_p » and the date of mid-duration «d_c» (Figure 3). There are three types of
174 hydrograph shapes: positive asymmetric if $d_p < d_c$, symmetric if $d_p = d_c$ and negative
175 asymmetric if $d_p > d_c$.

176 A hydrograph can be modeled by several methods such as the traditional unit
177 hydrograph method, (Pilgrim and Cordery, 1993), the synthetic unit hydrograph
178 method, (US-SCS, 1985), the typical hydrograph method, (Nezhikhovsky, 1971) and
179 the statistical method, (Ciepielowski, 1987; Haktanir and Sezen, 1990).

180 The statistical method is considered in present study where both Gamma and Beta
181 distributions were tested and it was concluded that, for the Baskatong watershed, Beta
182 distribution (with two parameters *a* and *b*) better reconstructs the shape of
183 hydrographs. The modeling methodology of the Beta distribution is explained in Yue
184 et al. (2002). The shape of the hydrograph is determined according to the ratio a/b:
185 positive asymmetry if $a/b < 1$, symmetry if $a/b = 1$ and negative asymmetry if
186 $a/b > 1$.

187 *Climb-rate:*

188 The climb-rate may be determined by the following equation (Young et al. 1999).

189 $$T_m = mean(t_i,\ i = d_s, ..., d_p) \qquad (4)$$

where t_i is the elementary climb-rate, d_s is the starting date and d_p is the peak date (Figure 2).

2.2 Statistical methods to analyze flood characteristics

In this section, we present the different statistical methods employed to analyze and compare flood characteristics. This section is composed of descriptive statistics, several correlations, stationarity, break-point detection and multivariate modeling.

Descriptive statistics:

In the descriptive part, we considered the mean and the variance of each characteristic and we plotted the corresponding box-plots. We used the Mann–Whitney test (Corder and Foreman, 2009) to check the significance of the difference between the compared mean series. To better explain the results, we superimposed the simulated and observed flood hydrographs. These hydrographs are presented for each year in Appendix D in Ben Aissia et al. (2009).

Correlations:

To investigate further the flood characteristics, three types of correlations are studied. The first is the correlation between different flood characteristics for the same series, the second is the correlation between different series of the same flood characteristic and the last one is the correlation between meteorological data and flood characteristics.

For space limitations, we considered the main flood characteristics: starting date « d_s », duration « D », peak « Qp » and volume « V ». For each value of the evaluated correlations, a statistical *t*-test (Kanji, 1993) was applied to check its significance.

Stationarity:

In order to study the stationarity of each one of the considered series, we applied the Mann-Kendall test (Mann, 1945 and Kendall, 1975). The Mann-Kendall test determines the existence of a trend in a series. The test statistic is given by:

$$Z = \begin{cases} \dfrac{S-1}{[\mathrm{var}(S)]^{1/2}} & if \quad S > 0 \\ 0 & if \quad S = 0 \\ \dfrac{S+1}{[\mathrm{var}(S)]^{1/2}} & if \quad S < 0 \end{cases} \tag{5}$$

where

$$S = \sum_{k=1}^{n-1} \sum_{j=k+1}^{n} \mathrm{sgn}\left(x_j - x_k\right) \tag{6}$$

and

$$\mathrm{sgn}(x) = \begin{cases} +1 & if \ x > 0 \\ 0 & if \ x = 0 \\ -1 & if \ x < 0 \end{cases} \tag{7}$$

If a series is detected as non-stationary by the Mann-Kendall test, then we apply to that series the modified Mann-Kendall test (Yue and Wang, 2002). This test completes the Mann-Kendall test by taking into account the autocorrelation in the series. Indeed, the presence of an autocorrelation affects the variance of the statistic *Z*. The modified test statistic *Z** is given by:

$$Z^* = \frac{Z}{\sqrt{\eta^*}} \tag{8}$$

where *Z* is the statistic of Mann-Kendall test given in (5) and η^* is a correction factor (see Yue and Wang, 2002).

Break-point:

To examine the existence of break-points in the series, we used the Bayesian method of multiple break-point detection in multiple linear regressions (Seidou and Ouarda, 2007). This method determines the number of break-points and their locations as well as the trends in each segment of the series. The Bayesian procedure assumes an improper noninformative prior as a distribution for the parameters representing the break-points. In the present study, the regression model is formulated as:

$$\begin{cases} y = \theta_1 x + \theta_2 + \varepsilon \text{ if } x \le \tau \\ y = \theta_1' x + \theta_2' + \varepsilon' \text{ if } x > \tau \end{cases} \quad (9)$$

where y represents the flood characteristic (e.g. peak), x is the time as years, $\theta_1, \theta_2, \theta_1'$ *and* θ_2' are the parameters to be estimated and τ is the break-point time.

Multivariate modeling

Copulas have received increasing attention in various fields of science. Copulas are used to describe the dependence structure between random variables. They are independent of marginal distributions. Therefore, the marginal distributions do not need to be the same. Three main flood characteristics (peak, volume and duration) are studied in a multivariate analysis. A copula is a p dimensional distribution function C ($p \ge 2$) with uniform margins on [0, 1]. Given such a copula, we can construct a multivariate distribution F with margins $F_{X_1},..,F_{X_p}$ through Sklar's (1959) theorem by:

$$F\left(x_1,..,x_p\right) = C\left(F_{X_1}(x_1),..,F_{X_p}(x_p)\right) \quad x_1,..,x_p \in R \quad (10)$$

Hence, fitting a multivariate distribution is divided into two parts: fitting a marginal distribution to each variable and fitting the dependence structure between

252 variables through copulas. On the other hand, copulas are employed to model the
253 dependence structure. In the literature, there are several copula families to model the
254 dependence structure between variables. The class of Archimedean copulas is widely
255 used in hydrology (Wong et al. 2008). For a convex decreasing function φ with $\varphi(1) =$
256 0, a copulas C_φ is said to be Archimedean with generator φ if C_φ can be expressed
257 in the form:

258 $$C_\varphi\left(u_1,..,u_p\right)=\varphi^{-1}\left(\varphi\left(u_1\right)+..+\varphi\left(u_p\right)\right)\ ;\ \ 0<u_1,u_2,...,u_p<1 \qquad (11)$$

259 where φ^{-1} represents the inverse of φ.

260 The most common Archimedean copulas are the copula of Gumbel, Frank and
261 Clayton. The goodness-of-fit test used is the graphical test proposed by Genest and
262 Rivest (1993) based on the *K* function given by:

263 $$K_\phi\left(u\right)=u-\frac{\phi\left(u\right)}{\phi'\left(u\right)};\ \ 0<u<1 \qquad (12)$$

264 ## 3. Results and discussion

265 All the considered flood characteristics are obtained for the different flow series.
266 Then, the results of the studied characteristics are analyzed at various levels, namely:
267 descriptive analysis, correlation study, stationarity study, break-point detection and a
268 multivariate analysis.

269 ### 3.1. Descriptive analysis of the results

270 In this section, we analyze the results of each characteristic in a descriptive
271 manner. To examine the ability of the used models to reproduce the observed
272 phenomena, we compare (RHS & RHY) and (SHS & SHY) to observed data. We then
273 compare SHSF and SHYF to SHS and SHY respectively in order to identify CC

274 effects. The descriptive statistics of the series of flood characteristics are gathered in
275 Table 2 and the corresponding the box-plots are in Figure 4.
276 For all considered flood characteristics, we check the significance of the difference
277 between compared series means by the Mann–Whitney test (Corder and Foreman,
278 2009).
279 *Starting date d_s:*
280 Figure 4a and Table 2 show that the starting dates of the simulated series RHS and
281 RHY are similar in the mean to those observed, but with larger variances. The starting
282 dates of the simulated series SHS and SHY occur later than those observed. However,
283 for the future series SHSF and SHYF, the starting dates could be earlier with more
284 variability.
285 *Ending date d_e:*
286 From Figure 4b and Table 2 we notice that for the HSAMI model, the ending
287 dates of the simulated series SHS and RHS are slightly later than those observed.
288 However, those simulated on the future period (SHSF and SHYF) have larger
289 variances.
290 *Duration D:*
291 The results presented in Figure 4c and Table 2 show that, except for the series
292 SHS, all other flood series simulated in the reference period have longer durations
293 than those observed. Comparisons between SHS and SHSF and between SHY and
294 SHYF show that future floods can be longer than those simulated in the reference
295 period. The series simulated by HYDROTEL have variances larger than those

296 simulated by HSAMI. The difference of variance can be explained by the fact that
297 HYDROTEL is a distributed model where simulated hydrographs can have a slightly
298 different shape than those simulated with HSAMI, a global model (Bisson and
299 Roberge, 1983).

300 *Flood peak Q_p:*

301 Figure 4d and Table 2 show that the flood peak could be lower and with less
302 variability in the future. Flood peaks simulated by HSAMI are higher than those
303 simulated by HYDROTEL. Neither hydrological model is able to simulate high flood
304 peaks as those observed in the historical data series.

305 *Peak date d_p:*

306 From Figure 4e and Table 2 we see that, with the exception of the series SHY,
307 peak date series are similar on average. For the future period, hydrological models
308 expect that the peak date would be earlier and more variable.

309 *Flood volume V:*

310 The results related to flood volume are presented in Figure 4f and Table 2. We can
311 observe that the flood volume series from the reanalysis data RHS is the only one to
312 provide a volume greater than that observed. In the future, flood volume can be bigger
313 and more variable. Flood volumes simulated by HSAMI are greater than those
314 simulated by HYDROTEL.

315 *Shape of the hydrograph F_h:*

316 Figure 4g and Table 2 show that the mean values of asymmetry coefficients
317 obtained are close to 1 for all series. Asymmetry coefficients obtained by

318 HYDROTEL are higher and more variable than those obtained by HSAMI. In
319 addition, we observe that the HSAMI model is not able to simulate the variation in the
320 shape of the hydrograph. The reason could be that, during the computation of water
321 discharge at the outlet, HSAMI uses only the Gamma distribution to model the shape
322 of the hydrograph (Bisson and Roberge, 1983).

323 *Climb-rate T_m:*

324 The results presented in Figure 4h and Table 2 related to the climb-rate of the
325 spring flood hydrograph show a possible increase of climb-rate and its variation in the
326 future. An opposition in the behavior of hydrological models HSAMI and
327 HYDROTEL between the reanalysis results (RHS, RHY) and simulations results
328 (SHS, SHY and SHSF, SHYF) is observed. Indeed, reanalysis results show that the
329 climb-rates simulated by HYDROTEL (RHY) are greater than those simulated by
330 HSAMI (RHS). The opposite is observed from the results of CGCM3.

331 *Peak of fall flood Q_{pa}:*

332 From Figure 4i and Table 2 we note that, except for the series SHYF, the
333 simulated series Q_{pa} by HSAMI are lower than those observed. However, the
334 simulated Q_{pa} series by HSAMI are lower than those simulated by HYDROTEL.
335 Comparisons between SHS and SHSF and between SHY and SHYF show that future
336 fall flood can be more important and with more variability.

337 Based on the results presented in this section, we concluded that the simulated
338 floods from RHS and RHY have later ending dates and longer duration than those
339 observed. Furthermore, the climb-rates of simulated floods from the reanalysis are

lower than those observed. For the simulated floods from SHS and SHY, we note that floods begin and end later than those observed and with fall peak, spring peak, volume and climb-rate lower than their observed counterparts. However, simulated floods from SHSF and SHYF could begin earlier than those simulated in the reference period and may have earlier peak. For HSAMI future flood could have longer duration and for HYDROTEL future flood could have larger climb-rate.

Comparison of the results of both hydrological models shows that the outputs from HYDROTEL have a variance greater than that of HSAMI. The volumes of the simulated flood by HSAMI are greater than those simulated by HYDROTEL whereas, the fall flood peaks simulated by HYDROTEL are greater than those simulated by HSAMI. On the other hand, from the reanalysis, simulated floods by HYDROTEL have climb-rate greater than those simulated by HSAMI. The opposite is observed from the results of CGCM3 on both periods. That is to say, for reference and future periods, the results of CGCM3 simulated floods by HSAMI have climb-rate greater than those simulated by HYDROTEL.

From Figures 4c and 4f we observe that generally the durations of simulated floods by HYDROTEL are longer than those simulated by HSAMI whereas the opposite holds for the volume. This result is not expected due to the usual positive correlation between V and D. This point will be studied in the next session.

3.2. Study of correlations

In this section, we analyze the correlations between the characteristics of the same series, between series of the same characteristic and between meteorological data and

362 different flood characteristics.

363 *Correlations between the characteristics of the same series*

364 Table 4 presents the correlations between the main flood characteristics for each
365 one of the seven considered series (DH, RHS, RHY, SHS, SHY, SHSF and SHYF).
366 We note that there is a strong negative correlation between the starting date and the
367 duration (between -0.47 and -0.72) and a strong positive correlation between the
368 volume and peak (between 0.44 and 0.70). The correlations between the *ds* and the
369 *Qp* and those between the *V* and *D* are less strong (about 0.3 to 0.4). Between the *V*
370 and the *ds* the correlations are low, generally below 0.2, and are considered not
371 significant. For correlations between *D* and *Qp*, three of the seven series have
372 moderate correlations (between -0.38 and -0.51) whereas the others have non
373 significant correlations (less than 0.30). These results are in agreement with those
374 generally obtained in the literature (e.g. Yue et al., 1999; Kim, 2003). Namely, there is
375 a correlation between both *V* and *Qp* and between *V* and *D* and not significant
376 correlation between *Qp* and *D*.

377 The moderate correlation between *V* and *D* can explain why in Figures 4c and 4f
378 the duration of HYDROTEL simulated floods are longer than those simulated by
379 HSAMI whereas the volume of HYDROTEL simulated floods are smaller than those
380 simulated by HSAMI.

381 *Correlations between series of the same characteristic*

382 For each of the four main characteristics considered, the correlations between the
383 seven series (DH, RHS, RHY, SHS, SHY, SHSF, and SHYF) are evaluated. The

corresponding results are presented in Table 5. The correlations are not significant for almost all series. Nevertheless the characteristic series from the reanalysis are correlated with the corresponding observed characteristics and the characteristic series simulated by HSAMI are correlated with those simulated by HYDROTEL.

Correlation between meteorological data and different flood characteristics

The hydrological models (HSAMI and HYDROTEL) have meteorological inputs series such as minimum temperature, maximum temperature and precipitation. Hence, these meteorological series and the characteristics of the simulated floods could be correlated. Moreover, in Québec spring flood is caused mainly by snow melting resulting from the increase in temperature during the spring. Therefore starting dates and maximum temperatures prior starting date could be correlated. Likewise, volume and precipitations could be correlated. First, we examine the correlation between the starting date and the average maximum temperatures of 7, 10 or 14 days prior the starting date. Then we evaluate the correlations between the starting date and the date when the maximum temperatures are always greater than zero. Finally, we calculated the correlation between volume and cumulative rainfall between December 15th and March 15th.

The results of correlations between the starting date and the average maximum temperature (Table 6) show that for five of the six series (except RHY) the correlation increases when the duration range increases. The opposite is observed in the series simulated by HYDROTEL (RHY). The starting date is moderately correlated with the date when the maximum temperature is always greater than zero (Table 7).

406 The correlation between the volume and the cumulative precipitation between
407 December 15th and March 15th (Table 8) is between 0.3 and 0.5 for the majority of the
408 series. The only exception is the series SHYF which gives a low correlation value.

409 **3.3. Stationarity**

410 The stationarity of all the considered series (63 series: 9 characteristic x 7 series)
411 is studied in this section using Mann-Kendall and modified Mann-Kendall tests. Table
412 9 shows the detected non-stationary series on the basis of the Mann-Kendall test. It
413 follows that among these series; two are actually slightly non-stationary using the
414 modified Mann-Kendall test: RHS and SHSF for the fall flood peak . These series are
415 both obtained from HSAMI. From Section 3.2, the two series RHS and RHY are
416 correlated (0.78) but only RHS is non-stationary. Similarly, the two series SHSF and
417 SHYF are correlated (0.83) but only SHSF is non-stationary. For a better comparison
418 of the two hydrological models (HSAMI and HYDROTEL), we represent the trends
419 associated with each of these four series of fall flood peak (RHS & RHY and SHSF &
420 SHYF) in Figure 5. We note that the slopes associated to the four identified trends are
421 positive. Series simulated by HYDROTEL have peaks higher than those simulated by
422 HSAMI and have a higher variability. In addition, the slopes of the series simulated
423 by HSAMI are larger than those simulated by HYDROTEL which explains the
424 non-stationarity detected in those simulated by HSAMI. Nevertheless, this
425 non-stationarity is weak given the large values of p-value (Table 9).

426 **3.4. Bayesian analysis for break-points detection**

427 The results of Bayesian analysis of break-points detection show that eight of the

428 considered series are identified with one break-point (Figure 6). These series are: the
429 *D* of SHSF and SHYF, the *V* of RHY, the *Fh* of SHY and SHS, the *Qpa* of DH and the
430 *Tm* of SHY and DH.

431 We note that on the reference period, the detected break-points are around the year
432 1985. Analysis of superimposed hydrographs shows that the period following 1985 is
433 a period characterized by low spring flow. Furthermore, in the future period two series
434 of duration (SHSF and SHYF) have a break-point in 2056. From Figure 6 we
435 conclude that the break amplitude is very slight. This break is caused, in the case of
436 the SHYF by an exceptional value simulated in 2055 (Figure 6) and, in the case of
437 SHSF, by a change of variation before and after the year 2055. The detection of this
438 break-point, with very slight amplitude, is related to the sensitivity of the employed
439 method (e.g. Beaulieu et al. 2009).

440 **3.5. Multivariate analysis**

441 To extend the study of flood characteristics, three main characteristics (peak,
442 volume and duration) are studied in a multivariate analysis. Fitting a multivariate
443 distribution is divided into two parts: fitting a marginal distribution to each variable
444 and fitting the dependence structure between variables through copulas.

445 *Adjustment of marginal distributions*

446 To determine the most appropriate marginal distribution to peak, volume and
447 duration, we used the HYFRAN software (Chaire en hydrologie statistique, 2002).
448 The choice of the appropriate distribution is based on the AIC criterion. The results of
449 marginal distribution are presented in Table 10. It can be seen that several

distributions adjust the series and we cannot draw a general conclusion on the marginal fittings.

Bivariate copulas

The fitting results are presented in Table 9 of the considered bivariate series. We observe that generally the Gumbel copula is more appropriate for peak-volume while that of Clayton is convenient for volume-duration.

4. Conclusions

The aim of this study is to evaluate and compare flood characteristics in a CC context. We used the historical flow data, the reanalysis data and the simulated data toward 2050. Both reanalysis and simulated data are obtained from two hydrological models HSAMI and HYDROTEL that used meteorological data from a CRCM. After evaluating and presenting the different flood characteristics associated to the considered series, a statistical study was conducted. This study involves a descriptive analysis of each characteristic, a study of different kinds of correlations, a stationarity analysis, detection of break-points and multivariate analysis.

The analysis of future flood characteristics shows that floods could begin earlier than those observed and could have earlier peaks. For HSAMI future floods could have longer durations and for HYDROTEL future floods could have larger climb-rates. The characteristic of the series simulated by HYDROTEL have larger variance than those simulated by HSAMI.

The correlations observed between the historical series are kept for both characteristics from reanalysis than for those from CGCM3 in the reference period.

We showed that most of the studied series are stationary except the two series RHS and SHSF for the peak of fall flood are very slightly non-stationary. The Bayesian method of break-point detection showed that eight of the 63 studied series have one break-point with slight magnitudes. For all the studied series, multivariate analysis of peak, volume and duration showed that the Gumbel copula is generally more appropriate for peak-volume whereas for volume-duration the Clayton copula represents generally a satisfactory fitting.

Although, in this study, most of the flood characteristics were considered and the study was conducted at various levels, some elements are not studied and should be considered. Indeed, the use of alternative future climate scenarios and more hydrological models could clarify the impacts of CC on flood characteristics. In the present study, we focused on comparing the reference and the future periods, the use of a moving average would allow for a complete comparison of the whole period. The use of other types of correlation such as Kendall's tau and Spearman's rho could give a better characterization of the relationship between the various flood characteristics. Furthermore, the use of other tests of break-point could improve our series analysis. It is also interesting to further study the multivariate frequency analysis including the concept of multivariate return period in order to quantify and compare the associated risks.

Acknowledgments

The authors thank the Natural Sciences and Engineering Research Council of Canada (NSERC) and Hydro-Québec for the financial support. The CRCM data has been

494 generated and supplied by Ouranos. The authors wish also to thank the
495 Editor-In-Chief and two anonymous reviewers whose comments helped improve the
496 quality of the paper.
497

References

Arnell, N.W. (1999). Climate change and global water resources. *Global Environnemental change*, 9: S31-S49.

Beaulieu, C., Seidou, O., Ouarda, T.B.M.J. and Zhang, X. (2009). Intercomparison of homogenization techniques for precipitation data continued: Comparison of two recent Bayesian change point models. *Water Resources Research*, 45 (8), art. no. W08410

Ben Aissia, M.A., Chebana, F., Ouarda, T.B.M.J., Roy, L., Desrochers, G., Chartier, I. et Robichaud, É. (2009). Analyse et comparaison des caractéristiques des crues historiques, résultats des réanalyses et simulées dans un contexte de changement climatique. Rapport de recherche, R-1074 *INRS-ETE*, Québec, Canada. P. 67. [In French]

Beniston, M. (2004). The 2003 heat wave in Europe: A shape of things to come? An analysis based on Swiss climatological data and model simulations. *Geophysical Research Letters*, 31 (2), L02202, doi:10.1029/2003GL018857.

Bergeron, L., Vigeant, G. and Lacroix, J, (1997). L'étude pancanadienne, Volume V: Impacts et adaptation à la variabilité et au changement du climat au Québec. *Environnement Canada, 279 p* [In French].

Bisson, J.L. and Roberge, F. (1983). Prévision des apports naturels: Expérience d'Hydro-Québec. Paper presented at the Workshop on flow predictions, Toronto [In French].

Brochu, R., and Laprise, R. (2007). Surface Water and Energy Budgets over the Mississippi and Columbia River Basins as Simulated by Two Generations of the Canadian Regional Climate Model. *Atmosphere-Ocean*, 45(1), 19-35.

Bruce, J., Burton, I., Martin, H., Mills, B. and Mortsch, L. (2000). Water Sector: Vulnerability and Adaptation to Climate Change. Final report submitted to the Climate Change Action Fund, Natural Resources Canada. Global Change Strategies International and Meteorological Service of Canada, *Downsview*, 141 p.

Chaire en hydrologie statistique (2002). HYFRAN. *Rapport technique*, INRS-ETE. Logiciel pour l'analyse fréquentielle en hydrologie, version 1.1 [In French].

Ciepielowski, A. (1987). Statistical methods of determining typical winter and summer hydrographs for engaged watersheds. *Flood hydrology*, V. P. Singh, ed., Reidel, Dordrecht, The Netherlands, 117– 124.

Corder, G.W. and Foreman, D.I. (2009). Nonparametric Statistics for Non-Statisticians: A Step-by-Step Approach. *New Jersey: Wiley*.

Cunderlik, J.M., and Ouarda, T.B.M.J., (2006). Regional flood-duration-frequency modeling in the changing environment. *Journal of Hydrology*, 318 (1-4): 276-291

D'Arcy, P., Bibeault, J..F. and Raffa, R. (2005). Changements climatiques et transport maritime sur le Saint-Laurent. Étude exploratoire d'options d'adaptation. Réalisé pour le Comité de concertation navigation du Plan d'action Saint-Laurent, *Ouranos*, 140 p [In French].

Dibike, Y.B. and Coulibaly, P. (2005). Hydrologic impact of climate change in the Saguenay watershed Comparison of downscaling methods and hydrologic models. *Journal of Hydrology*, 307 : 145-163.

Doré, I., Desrochers, G..É., Roy, R. and Chaumont, D. (2006). Les effets anticipés des changements climatiques sur les caractéristiques de crues - application à la rivière Moisie. L'association canadienne des barrages. *Ouranos*, 8 p [In French].

EEA (2008). Impacts of Europe's changing climate – 2008 indicator-based assessment. EEA Report. No. 4/2008.

Fortin, J.P., Moussa, R., Bocquillon, C. and Villeneuve, J.P. (1995). Hydrotel, un modèle hydrologique distribué pouvant bénéficier des données fournies par la télédétection et les systèmes d'information géographique. *Revue des Sciences de l'eau*, 8, 97-124. [In French]

Fortin, L.G., Turcotte, R., Plugin, S., Cyr, J.F. and Picard, F. (2007). Impact des changements climatiques sur les plans de gestion des lacs Saint-François et Aymer au Sud de Québec. *Canadian Journal of Civil Engineering*, 34(8): 934-945 [In French].

Genest, C. and Rivest, L.P. (1993). Statistical inference procedures for bivariate Archimedean copulas. *Journal of the American Statistical Association*, 88: 216-225.

Graham, L.P., Andréasson, J. and Carlsson, B. (2007). Assessing climate change impacts on hydrology from an ensemble of regional climate models, model scales and linking methods - A case study on the Lule River basin. *Climate change*, 81 : 293-307.

Guay, R., Mathieu, C., Fagherazzi, L., Tremblay, D., Desrochers, G. and Sassi, T. (2004). Analyse d'impacts des changements climatiques sur la rivière des Outaouais. *1er Symposium Ouranos sur les changements climatiques 9-10 juin 2004*. http://www.ouranos.ca/symposium/resume_PDF/Guay.pdf. Date of access: Novembre 2008 [In French].

Haktanir, T., and Sezen, N. (1990). Suitability of two-parameter gamma and three-parameter beta distributions as synthetic unit hydrographs in Anatolia. *Hydrological Science Journal*, 35(2) : 167–184.

Kanji, G.K. (1993). *100 Statistical Tests*. Sage Publications, London, Thousand Oaks, New Delhi. 216 p.

Kendall, M.G. (1975). *Rank Correlation Methods*, Griffin, London.

Khaliq, M.N., Ouarda, T.B.M.J., Gachon, P. and Sushama, L. (2008). Temporal evolution of low-flow regimes in Canadian rivers. *Water Resources Research*, 44 (8), art. no. W08436.

Kim, T., Valdés, J.B. and Yoo, C. (2003). Nonparametric approach for estimating return periods of droughts in arid region, *ASCE Journal of hydrologic Engineering*, 8 : 237-246.

Lorrain, K. (2007). Analyse des apports horizon 2050 pour les bassins Churchill Falls, Manic-5 et Caniapiscau, *Mémoire présenté à l'école de technologie supérieure, Montréal, Canada*. [in French]

585 Mann, H.B. (1945). Nonparametric tests against trend. *Econometric,* 13, pp. 245–259.
586 Mareuil, A., Leconte, R., Brissette, F. and Minville, M. (2007). Impacts of climate
587 change on the frequency and severity of floods in the Châteauguay River
588 basin, Canada. *Canadian Journal of Civil Engineering*, 34: 1048-1060.
589 Minville. M., Brisette, F. and Leconte, R. (2008). Uncertainty of the impact of climate
590 change on the hydrology of a Nordic watershed. *Journal of hydrology,* 358:
591 70-83.
592 Mortsch, L.D. and Quinn, F.H. (1996). Climate change scenarios for Great Lakes
593 Basin ecosystem studies, *Limnology and oceanography*, 41(5): 903-911
594 Music, B. and D., Caya. (2007). Evaluation of the Hydrological Cycle over the
595 Mississippi River Basin as Simulated by the Canadian Regional Climate
596 Model (CRCM). *Journal of Hydrometeorology*, 8(5), 969-988.
597 Nezhikhovsky, R. A. (1971). Channel network of the basin and runoff formation,
598 *Hydrometeorological*, Leningrad, Russia.
599 Ouarda, T.B.M.J., Rasmussen, P.F., Cantin, J..F., Bobée, B., Laurence, R., Hoang, V.D.
600 and Barabé, G. (1999). Identification of a hydrometric data network for the
601 study of climate change over the province of Quebec [Identification d'un
602 reseau hydrometrique pour le suivi des modifications climatiques dans la
603 province de Quebec]. *Revue des sciences de l'eau*, 12(2): 425-448.
604 Pachauri, R.K. (2002). L'évolution du climat. Les phénomènes météorologiques
605 extrêmes sont-ils un signe du changement climatique mondial. Online at
606 *http://www.un.org/french/pubs/chronique/2002/numero4/0402p58.html*. Date
607 of access: november 16 2009 [In French].
608 Pacher, G.W. (2006). Détermination objective des paramètres des hydrogrammes.
609 *Ouranos*, 8 p [In French].
610 Pilgrim, D.H., and Cordery, I. (1993). Flood runoff. Chapter 9 of Handbook of
611 hydrology, *D. R. Maidment, ed*., McGraw-Hill, New York. 1424 p.
612 Saint-Laurent, D., Mesfioui, M. and Even, G. (2009). Hydroclimatic variability and
613 relation with flood events (Southern Québec, Canada). *Water Resources*, 36
614 (1): 43-56.
615 Seidou, O. and Ouarda, T.B.M.J. (2007). Recursion-based multiple change-point
616 detection in multiple linear regression and application to river stream flows.
617 *Water Resources Research*, 43, W07404, doi: 10.1029/2006WR005021.
618 Singh B. (1987). Prospectives d'un changement climatique dû à un doublement de
619 CO2 atmosphérique pour les ressources naturelles du Québec, Rapport
620 préparé pour le service de l'Environnement atmosphérique (région du
621 Québec). *Environnement Canada*, 291 p [In French].
622 Sklar, A. (1959). Fonctions de répartition à n dimensions et leurs marges. *Publications*
623 *de l'Institut de statistique de l'Université de Paris*, vol. 8,p. 229–231.
624 U.S. Soil Conservation Service US-SCS (1985). *National Engineering Handbook*,
625 chap. Hydrology, U.S. Department of Agriculture., Washington, D. C. 600 p.
626 Vescovi, L., Cyr, J.F., Turcotte, R., Fortin, L.G., Ludwig, R., Braun, M. and May, I.
627 (2008). Rapport final du projet intitulé : Adaptation et inter comparaison
628 d'outils québécois et bavarois de gestion intégrée de bassins versants dans un

contexte de changements climatiques. *AQAGI*. 148 p [In French].

Warren, F.J. (2004). Climate change impacts and adaptation program: a Canadian perspective. *Ressources naturelles Canada*, 201 p.

Wilkinson, C. and Souter, D. (2008). Status of Caribbean coral reefs after bleaching and hurricanes in 2005. Global Coral Reef Monitoring Network, and Reef and Rainforest Research Centre, Townsville, 152 p.

Wong, G., Lambert, M.F. and Metcalfe, A.V. (2008). Trivariate copulas for characterisation of droughts. *Anziam Journal*, 9: C306-C323.

Young, W.J., Cuddy, S.M., Marston, F.M. and Farley, T.F.N. (1999). Environmental flows decision support system. Volume 1: system description. *CSIRO Land & Water Technical Report*, N°11/99, April 1999.

Yue, S., Ouarda. T.B.M.J., Bobée, B., Legendre, P. and Bruneau, P. (1999). The Gumbel mixed model for flood frequency analysis. *Journal of hydrology*, 226: 88–100.

Yue, S., Ouarda, T. B.M.J., Bobée, B., Legendre, P., and Bruneau, P. (2002). Approach for Describing Statistical Properties of Flood Hydrograph. *Journal of hydrologic engineering*, 7(2): 147-153.

Yue, S. and Wang, C.Y. (2002). Applicability of pre-whitening to eliminate the influence of serial correlation on the Mann-Kendall test. *Water resources research*, 38(6) : 1068, doi:10.1029/2001WR000861.

List of tables

List of Figures

678 # Tables

679 **Table 1 : Data series**

	Hydrological model	CRCM	Period	Notation
Observed	-	-	1971-2000	DH
Simulated	HSAMI	ERA-40	1971-2000	RHS
		CGCM3	1971-2000	SHS
			2040-2070	SHSF
	HYDROTEL	ERA-40	1971-2000	RHY
		CGCM3	1971-2000	SHY
			2040-2070	SHYF

680

681

682 **Table 2: Descriptive statistics of flood series characteristics**

Series		*DH*	*RHS*	*RHY*	*SHS*	*SHY*	*SHSF*	*SHYF*
d_s *(d)*	Mean	99	100	98	106	108	93	97
	Variance	91	123	146	151	86	167	220
	Minimum	80	76	71	81	91	66	57
	Maximum	115	118	120	130	125	117	128
d_e *(d)*	Mean	143	150	146	149	160	143	159
	Variance	99	64	112	83	114	170	254
	Minimum	116	130	123	128	146	114	113
	Maximum	161	163	166	168	187	163	195
D (d)	Mean	44	50	47	43	53	50	62
	Variance	133	55	180	148	232	155	314
	Minimum	22	36	25	27	28	25	38
	Maximum	66	65	85	81	79	81	125
Q_p (m^3s^{-1})	Mean	1282	1169	1094	991	774	979	740
	Variance	124820	45565	92538	77512	118980	83552	74343
	Minimum	672	761	567	459	230	326	268
	Maximum	2211	1576	1680	1678	1765	1641	1599
d_p *(d)*	Mean	117	119	117	119	134	108	118
	Variance	172	137	237	189	211	190	439
	Minimum	91	91	75	90	99	76	76
	Maximum	138	141	142	146	166	130	169
V (Mm^3)	Mean	3101	3389	2535	2400	2016	2522	2216
	Variance	585050	477310	487110	288440	485740	605370	663650
	Minimum	1565	2415	1472	1053	953	1226	881
	Maximum	5147	5105	3888	3175	4081	4321	3963
a/b	Mean	1.04	0.97	1.07	0.99	1.09	0.93	0.99
	Variance	0.01	0.01	0.02	0.01	0.02	0.01	0.04
	Minimum	0.86	0.72	0.85	0.85	0.75	0.65	0.53
	Maximum	1.24	1.15	1.60	1.21	1.46	1.11	1.33
T_m $(m^3s^{-1}d^{-1})$	Mean	25	21	28	23	10	28	14
	Variance	74	47	97	22	14	58	13
	Minimum	7	9	9	12	3	15	8
	Maximum	39	32	45	31	18	44	21
Q_{pa} (m^3s^{-1})	Mean	550	397	540	329	480	440	595
	Variance	68406	14801	32707	12892	16090	33967	79649
	Minimum	204	182	275	172	301	196	262
	Maximum	1402	655	1046	636	855	916	1453

683
684

685 **Table 3 : p-value of the Mann-Whitney test**

	DH&RHS	DH&RHY	DH&SHS	DH&SHY	RHS&SHS	RHY&SHY	SHS&SHSY	SHY&SHYF
d_s	0.66	0.75	0.02	0.00	0.06	0.00	0.00	0.00
d_e	0.01	0.59	0.03	0.00	0.75	0.00	0.11	0.58
D	0.04	0.36	0.59	0.04	0.00	0.20	0.02	0.06
Q_p	0.37	0.07	0.00	0.00	0.01	0.00	0.98	0.80
d_p	0.55	0.97	0.66	0.00	0.86	0.00	0.01	0.00
V	0.14	0.01	0.00	0.00	0.00	0.00	0.70	0.33
F_h	0.01	0.84	0.03	0.20	0.38	0.30	0.02	0.02
T_m	0.06	0.16	0.16	0.00	0.32	0.00	0.09	0.00
Q_{pa}	0.01	0.74	0.00	0.46	0.01	0.19	0.01	0.19

686 **The gray color indicates that the corresponding mean difference is significant.**

687

688 **Table 4 : Correlations between main flood characteristics**

	D		Q_p		V	
d_s	-0.57		0.30		-0.03	
	-0.69	-0.66	0.33	0.22	0.06	-0.16
	-0.72	-0.72	0.58	0.39	0.14	-0.11
	-0.47	-0.53	0.11	-0.18	-0.13	-0.45
D	1		-0.28		0.46	
			-0.14	-0.38	0.32	0.46
			-0.46	-0.51	0.17	0.27
			-0.28	-0.15	0.36	0.60
Q_p	DH		1		0.61	
	RHS	RHY			0.68	0.44
	SHS	SHY			0.70	0.57
	SHSF	SHYF			0.68	0.55

689 Example: -0.57 is the correlation between the duration and starting date which are determined from the series of
690 historical data.

691 The gray color indicates that the corresponding correlation is significant.

692

693 **Table 5: Correlations between simulated and historical series**

	RHS		*RHY*		*SHS*		*SHY*		*SHSF*		*SHYF*	
DH	0.84	0.59	0.79	0.37	0.21	-0.07	0.12	-0.03	0.00	-0.13	-0.02	-0.17
	0.47	0.59	0.36	0.49	-0.02	-0.12	0.00	-0.03	0.10	-0.01	0.20	-0.21
RHS	1		0.95	0.85	0.13	0.15	0.04	-0.04	-0.03	-0.17	-0.18	-0.31
			0.69	0.88	0.23	0.21	0.38	0.08	0.26	-0.05	0.14	-0.04
RHY			1		0.10	0.15	-0.02	-0.09	-0.01	-0.13	-0.16	-0.20
					0.12	0.18	0.29	-0.05	0.31	-0.04	0.24	-0.02
SHS					1		0.91	0.53	-0.05	-0.23	0.05	-0.11
							0.86	0.56	0.24	0.17	0.19	0.13
SHY			**d_s**	**D**			1		-0.23	-0.13	-0.04	-0.17
			Q_p	**V**					0.21	-0.12	0.18	0.00
SHSF									1		0.73	0.31
											0.80	0.70

694 Example: 0.85 is the correlation between the duration series determined from RHY and RHS

695 The gray color indicates that the corresponding correlation is significant.

696

697

Table 6 : Correlation between starting date and average maximum temperature.

	Average maximum temperature		
Series	7 days	10 days	14 days
RHS	0.26	0.37	0.54
SHS	0.44	0.59	0.69
SHSF	0.33	0.41	0.53
RHY	0.38	0.36	0.18
SHY	0.28	0.39	0.44
SHYF	0.33	0.39	0.44

The gray color indicates that the corresponding correlation is significant.

Table 7 : Correlations between the starting date and the date of the maximum temperature are always greater than zero

Starting date series	Date from which the maximum temperature are always greater than zero
RHS	0.45
SHS	0.64
SHSF	0.49
RHY	0.33
SHY	0.57
SHYF	0.55

The gray color indicates that the corresponding correlation is significant.

706 **Table 8 : Correlation between the flood volume and the cumulative of rainfall**
707 **between December 15th and March 15th**

Series	Correlation
RHS	0.42
SHS	0.31
SHSF	0.51
RHY	0.37
SHY	0.41
SHYF	0.17

708 The gray color indicates that the corresponding correlation is significant.
709
710

711 **Table 9 : Stationarity tests of the characteristics**

		Mann-Kendall			Modified Mann-Kendall		
Characteristics	Series	K	p-value	Significant Trend	K	p-value	Significant Trend
Climb-rate	DH	2.29	0.02	yes	1.07	0.28	no
	RHS	2.56	0.01	yes	1.50	0.13	no
	RHY	2.65	0.01	yes	0.46	0.64	no
	SHSF	3.11	0.00	yes	1.54	0.12	no
Fall flood	RHS	2.51	0.01	yes	2.45	0.01	yes
	SHSF	2.85	0.00	yes	2.00	0.05	yes

712

713 **Table 10 : Parameters of marginal distribution series of peak, volume and**
714 **duration**

Characteristic	*Series*	*Marginal distribution*	*Parameter*		
			α	*β*	*σ*
Q_p	HD	Gumbel	1123.0	275.5	
	RHS	Gamma	30.7	38.0	
	RHY	Weibull	4.1	1206.6	
	SHS	Fuites	38.0	26.1	
	SHY	Fuites	73.4	12.6	
	SHSF	Fuites	42.6	23.0	
	SHYF	Gamma	8.0	96.0	
V	HD	Gamma	17.0	182.6	
	RHS	Gumbel	3077.6	538.7	
	RHY	Log-Normal (two parameters)	606.1	0.7	
	SHS	Generalized extreme value	2314.1	7.8	0.3
	SHY	Gumbel	1701.3	543.4	
	SHSF	Fuites	116.6	21.6	
	SHYF	Gamma	7.4	298,0	
D	HD	Fuites	1.5	30.1	
	RHS	Halphen type B	49.4	2.0	14.71
	RHY	Gamma	12.7	3.7	
	SHS	Gumbel	37.9	8.8	
	SHY	Gamma	11.9	4.4	
	SHSF	Gamma	16.5	3.0	
	SHYF	Gumbel	54.0	11.6	

715 Where α is the parameter position for the distributions: Gumbel, Weibull, Fuites, GEV and Log-Normale (two
716 parameters) and the shape parameter for the distributions: Gamma and Halphen type B. While β represents the
717 scale parameter for the distributions: Gumbel, Gamma, Weibull, GEV, Log-Normale (two parameters) and
718 Halphen type B and the shape parameter for the fuites distributions. Finally, σ is the shape parameter for the
719 distributions GEV and Halphen type B

720 **Table 11 : Bivariate copulas fitted to peak-volume and volume-duration**

	DH	RHS	RHY	SHS	SHY	SHSF	SHYF
Peak-Volume	Gumbel	Gumbel	Fank	Gumbel	Gumbel	Gumbel	Clayton
Volume-Duration	Clayton	Clayton	Fank	Clayton	Clayton	Gumbel	Gumbel

721

722

Figures

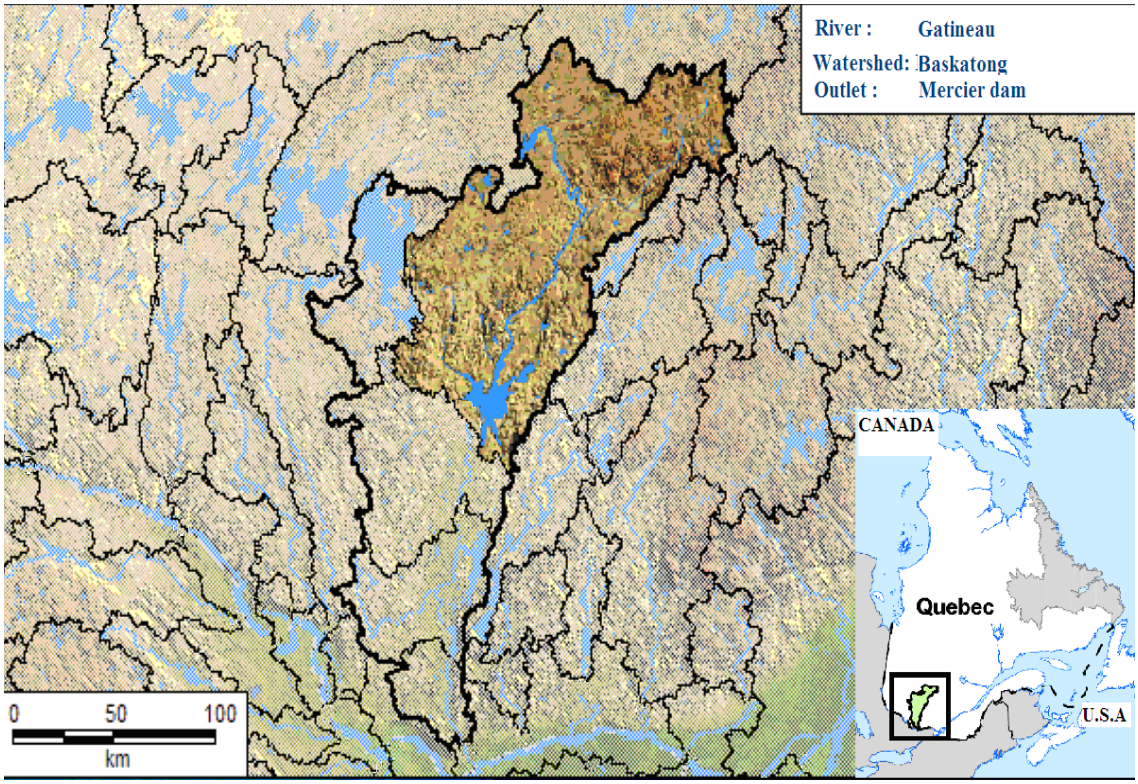

Figure 1 : Watershed of the Baskatong reservoir map location

727

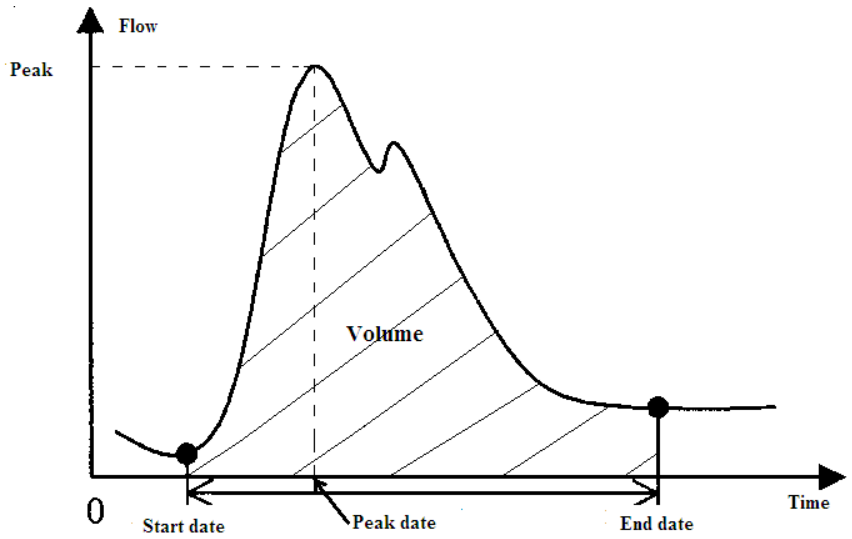

728

729 **Figure 2 : Different characteristics of a hydrograph.**

730

731

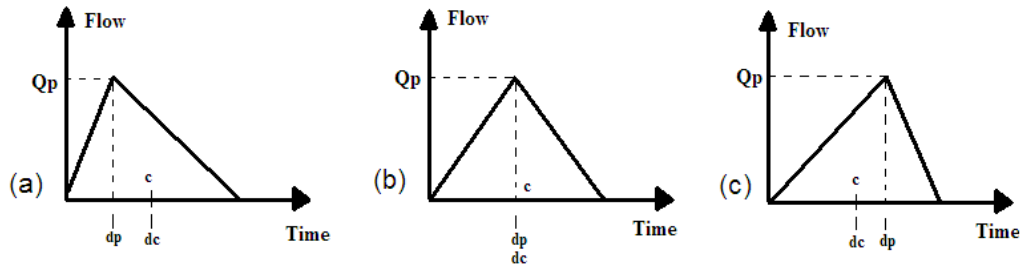

732

733 **Figure 3 : Diagram illustrating the three types of shape of hydrograph: (a)**

734 **positive asymmetry (b) symmetry (c) negative asymmetry.**

735

736

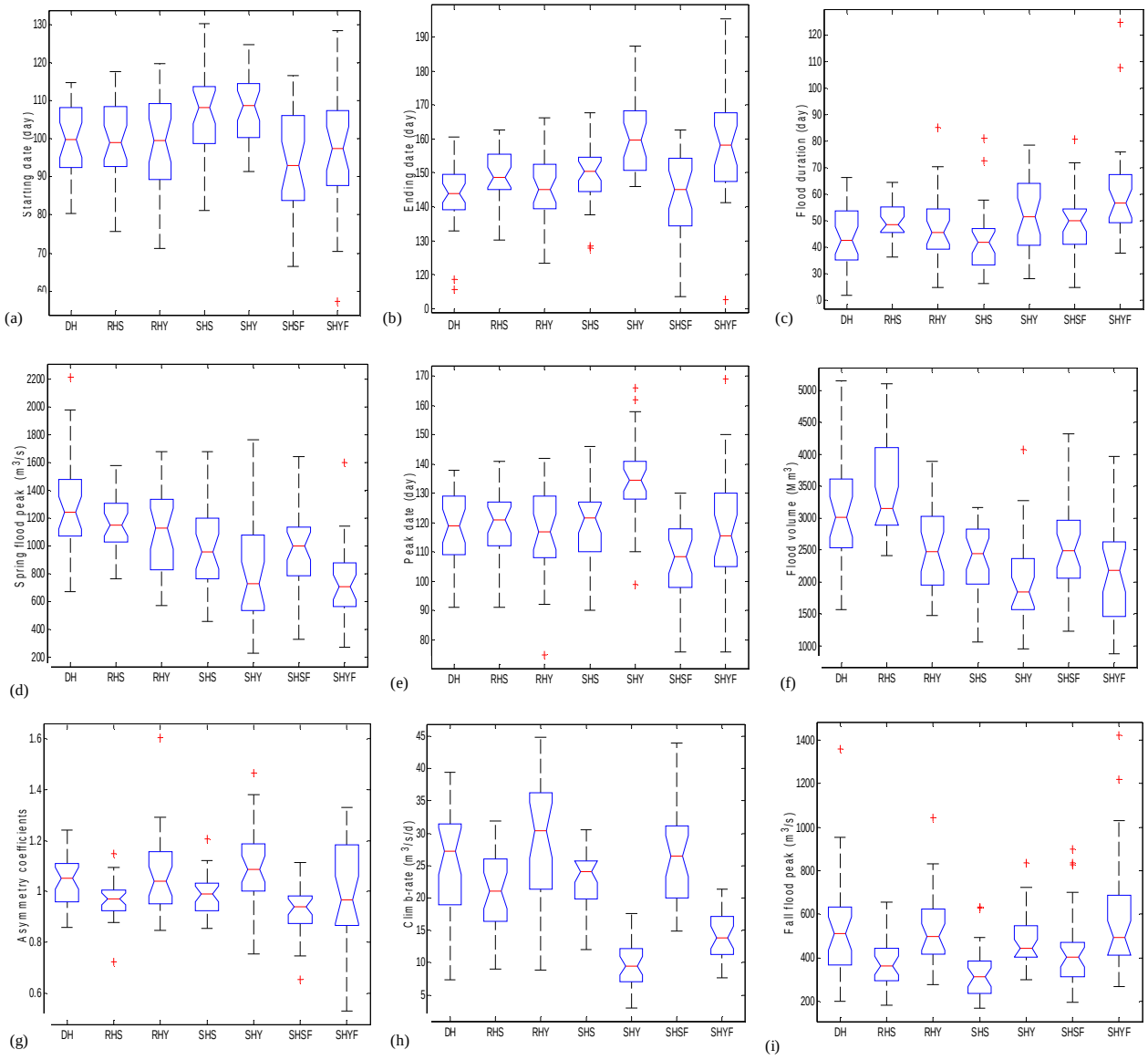

737 **Figure 4: Box-plot flood characteristics series: a) starting date, b) ending date, c) duration,**

738 **d) peak, e) peak date, f) volume, g) asymmetry coefficient, h) climb-rate and i) fall flood peak**

739

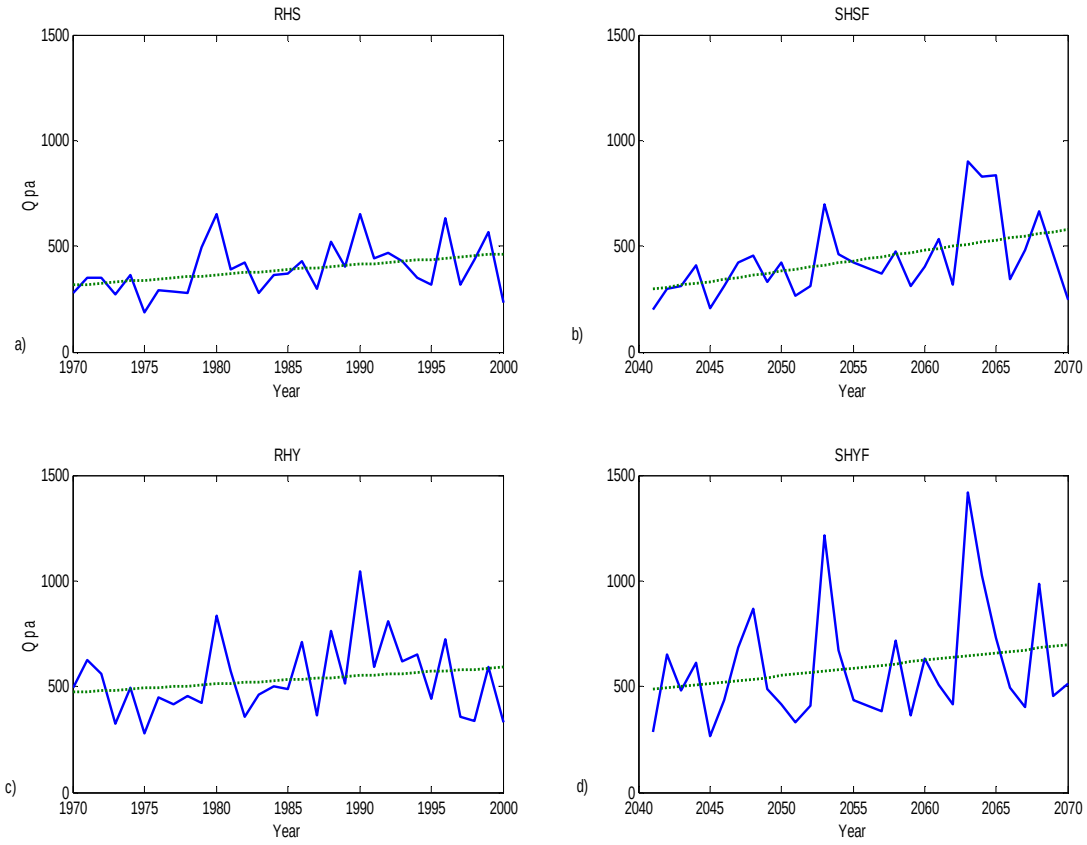

Figure 5 : Non-stationary in fall flood peak and associated trends: a) RHS, b) SHSF, c) RHY and d) SHYF. The dashed line represents the corresponding trend of each series.

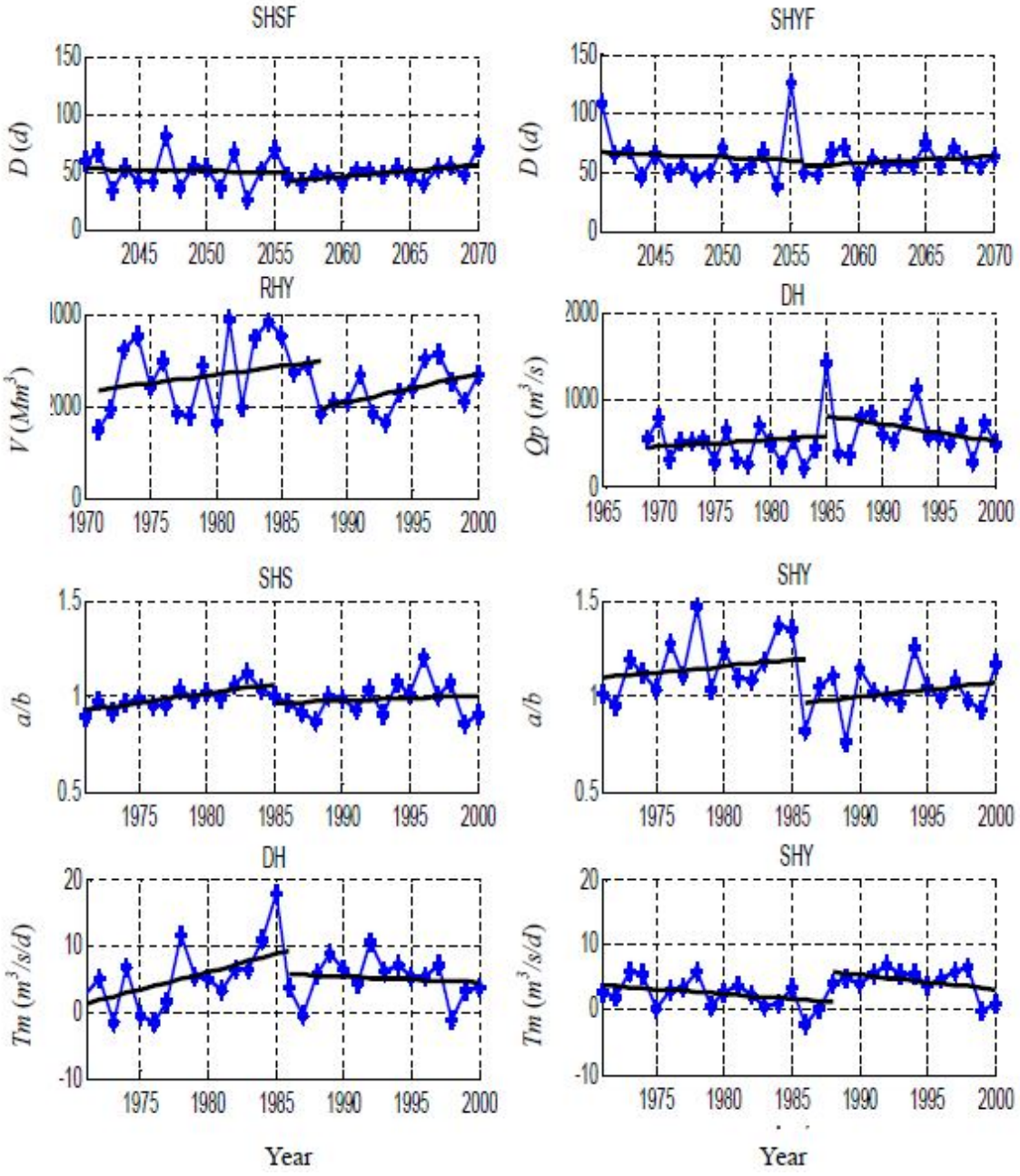

Figure 6: Detected break-points in the considered series